

1 **Effect of Fuel Injection Pressure and Injection**
2 **Timing of Karanja Biodiesel Blends on Fuel**
3 **Spray, Engine Performance, Emissions and**
4 **Combustion Characteristics**

5
6 **Avinash Kumar Agarwal^{a*}, Atul Dhar^a, Jai Gopal Gupta^a,**

7 **Woong Il Kim^b, Kibong Choi^b, Chang Sik Lee^b, Sungwook Park^b**

8 ^aEngine Research Laboratory^a, Department of Mechanical Engineering,

9 Indian Institute of Technology Kanpur, Kanpur-208016, India

10 ^bCombustion Engine and Energy Conversion Laboratory^b

11 School of Mechanical Engineering, College of Engineering, Hanyang University

12 Seoul 133-791, Republic of Korea

13 *Corresponding Author's email: akag@iitk.ac.in

14
15 **Abstract**

16 In this investigation, effect of 10, 20 and 50% Karanja biodiesel blends on injection rate,
17 atomization, engine performance, emissions and combustion characteristics of common
18 rail direct injection (CRDI) fuel injection system were evaluated in a single cylinder
19 research engine with CRDI at 300, 500, 750 and 1000 bar fuel injection pressures at
20 different start of injection timings and constant engine speed of 1500 rpm. The
21 duration of fuel injection slightly decreased with increasing blend ratio of biodiesel
22 (Karanja Oil Methyl Ester: KOMe) and significantly decreases with increasing fuel
23 injection pressure. The injection rate profile and sauter mean diameter (D_{32}) of the fuel

24 droplets are influenced by the injection pressure. Increasing fuel injection pressure
25 generally improves the thermal efficiency of the test fuels. Sauter mean diameter (D_{32})
26 and arithmetic mean diameter (D_{10}) decreased with decreasing Karanja biodiesel
27 content in the blend and significantly increased for higher blends due to relatively
28 higher fuel density and viscosity. Maximum thermal efficiency was observed at the same
29 injection timing for biodiesel blends and mineral diesel. Lower Karanja biodiesel blends
30 (upto 20%) showed lower brake specific hydrocarbon (BSHC) and carbon monoxide
31 (BSCO) emissions in comparison to mineral diesel. For lower Karanja biodiesel blends,
32 combustion duration was shorter than mineral diesel however at higher fuel injection
33 pressures, combustion duration of 50% blend was longer than mineral diesel. Upto 10%
34 Karanja biodiesel blends in a CRDI engines improves brake thermal efficiency and
35 reduces emissions, without any requirement of hardware changes or ECU recalibration.
36 **Keywords:** Combustion; Karanja biodiesel; Emissions; Fuel injection pressure;
37 Injection timing.

38

39 **1. Introduction**

40 Diesel engines are extensively used and dominating power sources for road transport
41 sector due to their higher thermal efficiency, operational reliability, robustness, lower
42 hydrocarbon (HC) and carbon monoxide (CO) emissions. In the last two decades,
43 biodiesel has emerged as a well-accepted alternative fuel to mineral diesel because its
44 utilization requires insignificant modifications in the engine hardware. With advanced
45 fuel injection systems, fuel injection pressures have risen by an order of magnitude in
46 comparison to older mechanical fuel injection systems. It is therefore very important to
47 investigate the effect of fuel injection pressure on comparative performance, emissions
48 and combustion characteristic of biodiesel and mineral diesel for effective utilization of
49 biodiesel in modern CI engines. Boudy *et al.* estimated the influence of fuel properties on

50 the pressure–wave in the injector feed pipe and injector mass flow rate by the modeling
51 for a common-rail diesel injection system and reported that amount of injected mass was
52 mainly affected by the density of the fuel [1]. Yehliu *et al.* observed 12% higher brake
53 specific fuel consumption (BSFC) for B100 (with 15% lower calorific value than diesel) in
54 comparison to mineral diesel in a four-cylinder CRDI engine [2]. Suryawanshi *et al.*
55 reported slightly higher brake thermal efficiency (BTE) for *Pongamia* biodiesel blends in
56 comparison to mineral diesel. They also reported that retarding the injection timing by 4
57 crank angle degrees resulted in minor improvement in thermal efficiency at part loads
58 and no change at full load [3]. Grimaldi *et al.* obtained slightly higher engine efficiency,
59 when the engine was fuelled with biodiesel, particularly at high load in comparison to
60 mineral diesel fuelled engine [4]. Zhu *et al.* reported that oxygenated fuels including
61 biodiesel, biodiesel-ethanol and biodiesel-methanol blends gave better BTE at all engine
62 operating conditions vis-à-vis mineral diesel [5]. Gumus *et al.* observed that BTE of
63 mineral diesel decreased as fuel injection pressures increased from 18 to 24 MPa but for
64 biodiesel, it increased with increasing fuel injection pressure at full load [6]. Highest
65 achieved BTE for diesel (at 18 MPa injection pressure) and biodiesel (at 24 MPa
66 injection pressure) were 32.1 and 41.3% respectively [6]. Agarwal *et al.* reported that
67 higher fuel injection pressure leads to a longer spray tip penetration and larger spray
68 area compared to lower fuel injection pressures after identical elapsed time after the
69 start of injection (SOI) for Karanja biodiesel blends and diesel [7].
70 Baldassarri *et al.* reported 10% reduction in CO emissions by fuelling the bus engines by
71 B20 vis-à-vis mineral diesel [8]. Zhu *et al.* observed lower BSCO emissions for biodiesel
72 fuelled engine in comparison to diesel fuelled engine [5]. Kousoulidou *et al.* observed
73 that biodiesel does not have any effect on CO emission levels vis-à-vis mineral diesel in
74 an engine equipped with common rail injection system [9]. Suh *et al.* reported reduction
75 in CO emissions for biodiesel blends as well as mineral diesel with advanced injection

76 timing [10]. Wang *et al.* observed that 35% soybean biodiesel blend resulted in reduced
77 HC emissions in comparison to mineral diesel [11]. Gumus *et al.* reported that NO_x
78 emissions generally decreased with increasing fuel injection pressure but the trend was
79 not regular and significant [6].

80 Kuti *et al.* investigated the spray formation and combustion characteristics of Palm
81 biodiesel and mineral diesel by using a CRDI system in a constant volume chamber [12].
82 They observed longer liquid length for biodiesel in comparison of mineral diesel due to
83 higher boiling range of biodiesel [12]. Ignition delay (ID) was shorter for biodiesel due to
84 its higher cetane number. ID reduced with increasing fuel injection pressure and
85 decreasing nozzle diameter [12]. Suh *et al.* reported similar combustion pressure and
86 rate of heat release for 5% blend of soybean biodiesel and mineral diesel [10]. Lee *et al.*
87 investigated the effect of biodiesel blended fuels (Biodiesel derived from unpolished rice
88 and soyabean) on the atomization and combustion characteristics for a common-rail
89 single-cylinder engine. It was reported that higher surface tension and viscosity of the
90 biodiesel causes lower Weber number and decreases injection velocity of biodiesel-
91 blended fuels respectively, and result in increased mean droplet size diameter with
92 increasing blend ratio. The spray tip penetration was observed to be longer for higher
93 injection pressure. Higher cetane number of biodiesel causes shorter ignition delay,
94 which was responsible for increased peak combustion pressure with an increase of the
95 biodiesel blend ratio. With increasing biodiesel blend ratio, lower HC and CO were
96 observed, whereas NO_x emissions increased, possibly because of fuel oxygen in biodiesel
97 coupled to shorter ignition delay of biodiesel. [13]. Experimental study by Can concluded
98 that despite earlier start of injection, combustion and engine performance
99 characteristics proved that the ignition delay decreased with addition of biodiesel at all
100 engine loads with relatively earlier SOC due to higher cetane number of biodiesel [14].

101

102 Depending upon the local availability, different feedstocks are being promoted
103 worldwide for production of biodiesel. Biodiesel policy of India encourages utilization of
104 non-edible oils for biodiesel production because India has shortage of edible oils [15].
105 Karanja also known as *pongamia pinnata*, is a tree borne oil seed, which naturally
106 grows in almost whole of south Asia [16-18]. Karanja is one of the important nitrogen
107 fixing trees (NFTs) which produces seeds containing 30-40% oil (w/w). It is planted as an
108 ornamental and shade tree but now-a-days, it has emerged as an important resource for
109 oil, which can be used for production of biodiesel. The average seed yield of Karanja is
110 about 4-9 tons/ha [19]. Based on review of several experimental studies, Ashraful *et al.*
111 concluded that Karanja biodiesel is superior because of its cetane number, higher brake
112 thermal efficiency, lower BSFC and lower emission characteristics in comparison to
113 various other non-edible feedstock based biodiesels [20]. Its utilization for large scale
114 biodiesel production will ensure stability of supply because it is well adapted to local
115 climatic conditions. In this study, effect of Karanja biodiesel blends on engine
116 performance, emissions and combustion characteristics have been experimentally
117 investigated at different fuel injection pressure for exploring the prospects of Karanja
118 biodiesel/ blends utilization in modern transport engines equipped with common rail
119 direct injection (CRDI) fuel injection system. In addition to detailed engine
120 investigations, spray studies have also been done.

121

122 **2. Experimental Setup**

123 **2.1 Injection rate and spray droplet measuring system**

124 In order to investigate the injection rate of Karanja oil biodiesel, the injection rate
125 measuring system was used for various injection pressure conditions as illustrated in
126 Figure 1. This system is based on the pressure variation in a measuring tube, filled with
127 biodiesel. When the high- pressure biodiesel is injected into the tube, the fuel creates

128 pressure wave detected by a pressure sensor in the tube. During the fuel injection, the
 129 pressure in the tube was maintained constant at 20 bar. In the system, the line pressure
 130 was continuously measured by using the pressure sensor. In this test, 1000 fuel
 131 injections were carried out and the measurements were averaged.

132 Figure 2 shows the phase Doppler droplet analysis system, which comprises of a high-
 133 pressure fuel injection system, an Ar-Ion laser, a transmitter, a receiver, data
 134 acquisition and signal synchronizer system. To investigate the droplet size of Karanja
 135 biodiesel under varying injection pressure conditions, droplet measuring system with a
 136 514.5 nm and 488 nm wavelengths were applied. As listed in Table 1, photomultiplier
 137 voltages and laser output were selected at 500V and 700mW, respectively. For
 138 measuring range of droplet size, cut-off range of the droplet sizes for spray measurement
 139 was set up from 2 μm to 75 μm . In this investigation, a 0.3 mm single hole nozzle with
 140 0.8 mm hole depth was used in order to the prevent the interference of droplet
 141 coalescence between neighboring droplets due to multi-hole nozzle.

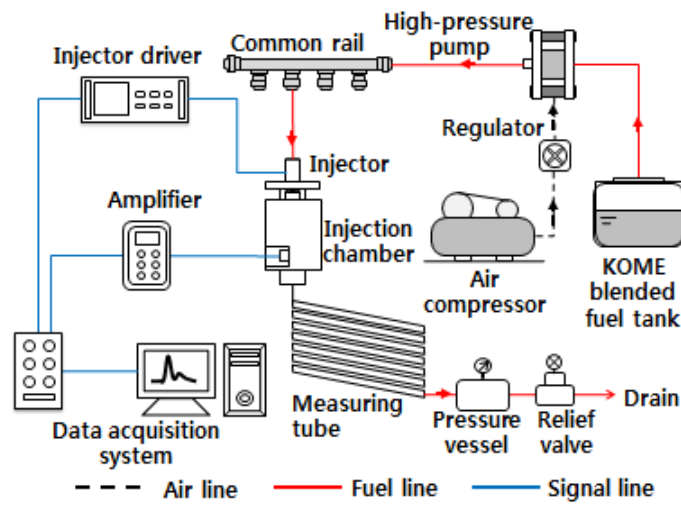
142 Table 1: Details of injection rate and spray droplet measurement systems

Injection rate measurement system	Fuel injection system	Common rail direct injection
	Injection rate meter	Bosch's procedure [21-23]
	Fuel injection pressure (bar)	300-1000
	Number of nozzle holes	6
	Nozzle hole diameter (mm)	0.131
	Measuring tube pressure (bar)	30
	Injected mass (mg)	12
Droplet measurement system	Light source	Ar-ion laser
	Wave length (nm)	514.5 nm, 488 nm
	Focal length (mm)	Transmitter: 500, Receiver: 250
	Collection angle (degrees)	30

	Fuel injection pressure(bar)	600-1000
	Number of holes	1
	Nozzle hole diameter (mm)	0.3
	Injected mass (mg)	12

143

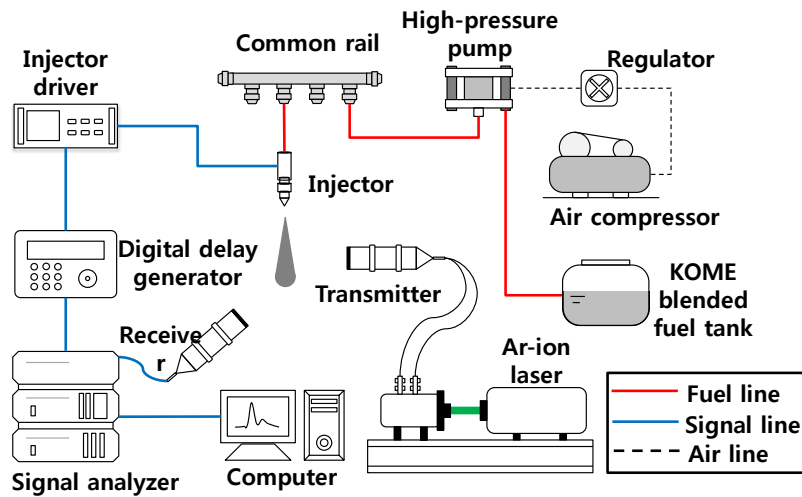
144



145

146

(a) Injection rate measuring system



147

148

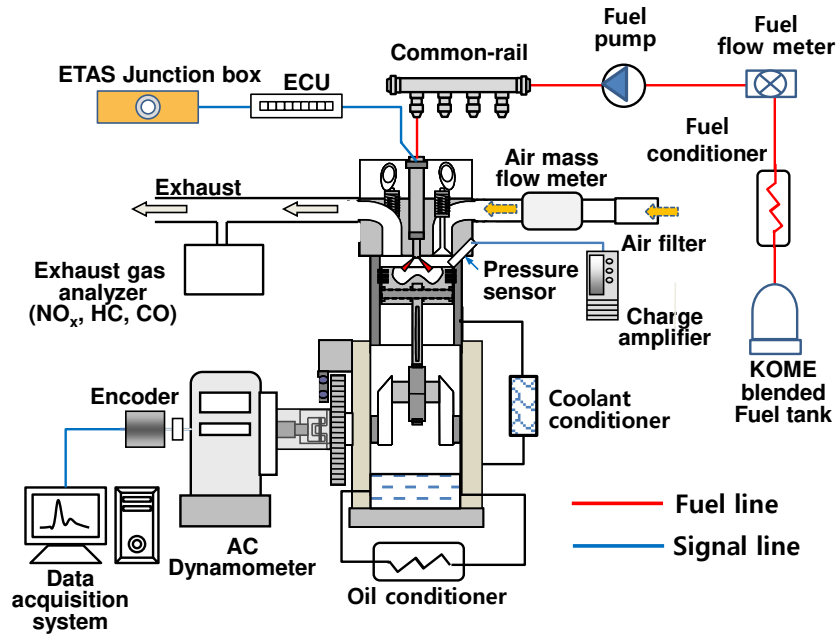
(b) Phase Doppler particle analyzer system

149

Figure 1: Injection rate and phase Doppler particle analyzer system

150 Schematic of the experimental setup used for evaluation of engine performance,
151 emissions and combustion characteristics of test fuels at different fuel injection
152 pressures is shown in Figure 2.

153



154

155 Figure 2: Schematic of the engine experimental setup

156 Effect of fuel injection pressure (FIP), start of injection (SOI) timing and injection
157 strategy on the engine performance, emissions and combustion characteristics were
158 evaluated using a single cylinder research engine (AVL List GmbH; 5402). This test
159 engine was equipped with a common rail direct injection (CRDI) system. Detailed
160 technical specifications of the test engine are given in Table 2. Engine performance,
161 emissions and combustion characteristics of the test engine were investigated at 300,
162 500, 750 and 1000 bar FIPs and varying SOI timings. During the experiments, fuel
163 temperature was maintained at 20°C using fuel conditioning unit (AVL List GmbH;
164 753CH). For these experiments, engine management system was operated in manual
165 mode with user defined control of FIP, SOI timings and injected fuel quantity.
166 Lubricating oil temperature and pressure were also maintained at 90°C and 3.5 bar

167 respectively using an oil condition system (Yantrashilpa; YS4312). Coolant temperature
168 was kept maintained at 80°C by coolant conditioning condition unit (Yantrashilpa;
169 YS4027).

170 Air and fuel consumption rates were measured by rotary gas flow meter system (Elster
171 Instromart; RVG G160) and a fuel flow meter (AVL List GmbH; Fuel Balance 733S.18)
172 respectively. Raw engine emissions were measured by exhaust gas emissions analyser
173 (AVL List GmbH; 444). Exhaust gas sample was passed through a moisture trap and a
174 filter to arrest moisture condensation and particulates from entering the analyzer test
175 cell. HC is measured in 'ppm of hexane equivalent'; NO measured in 'ppm' and CO, CO₂,
176 and O₂ are measured in 'volume percentage'. Accuracy and measurement ranges of
177 emission analyzer have been given in table 3. For comparison across different power
178 ranges, data of raw emissions from the exhaust gas emission analyzer is converted to
179 mass emissions i.e. brake specific emission using IS: 14273 code [24]. Cylinder pressure
180 was measured by a water cooled piezoelectric pressure transducer (AVL List GmbH;
181 QC34C) mounted flush in the cylinder head. Rotation of the crank shaft was recorded by
182 an optical encoder (AVL List GmbH; 365CC/ 365X). For acquisition and analysis of
183 cylinder pressure-crank angle data, a high speed data acquisition system (AVL List
184 GmbH; Indismart-611) was used. Variation in cylinder pressure with crank angle was
185 recorded for 200 consecutive engine cycles and then averaged for eliminating the effect
186 of cycle-to-cycle variations. This averaged cylinder pressure data was used to calculate
187 heat release rate, mass-burn fraction crank angles, combustion duration and other
188 combustion related parameters.

189 Experiments were performed for mineral diesel, biodiesel and three biodiesel blends
190 (KOME10, KOME20 and KOME50) at constant engine speed (1500 rpm). Important
191 physical properties of test fuels are given in Table 4. Fuel energy injected into each
192 engine cycle was kept constant for all engine operating conditions, which was equivalent

193 to air-fuel ratio (AFR) of 23 using mineral diesel. Engine operating point corresponding
 194 to 5 bar brake mean effective pressure (BMEP) engine load and 1500 rpm engine speed
 195 was chosen for detailed investigations of the effect of FIP and SOI timings on particulate
 196 numbers emitted. Upper limit of advanced SOI timings at each FIPs was limited by
 197 peak rate of pressure rise limit (15 bar/deg). Lower limit of retarded SOI timings was
 198 limited by the lower selected limit of BMEP (4.5 bar).

199 Table 2: Specifications of the test engine

Engine Make, Model	AVL 5402
Number of cylinders	1
Cylinder bore/ stroke (mm)	85/ 90
Swept volume (cc)	510.7
Compression ratio	17.5
Number of valves	4
Inlet ports	Tangential and swirl inlet port
Maximum power (kW)	6
Fuel injection system	Common rail direct injection
Fuel injection pressure (bar)	200-1400

200

201 Table 3. Measurement range, resolution and accuracy of the exhaust gas

202 emission analyzer (AVL444)

Species	Range	Resolution	Accuracy
CO	0-10% vol.	0.01 vol. %	<0.6% vol.: ±0.03% vol. ≥0.6% vol.: ± 5% of ind. vol.
CO ₂	0-20% vol.	0.1 vol. %	<10% vol.: ±0.5% vol. ≥10% vol.: ± 5% of ind. vol.
HC	0-20000 ppm	≤ 2000:1 ppm vol. ≤ 2000:10 ppm vol.	<200ppm vol.: ± 10 ppm vol. ≥200ppm vol.: ± 5% of ind. vol.
NO	0-5000 ppm	1 ppm vol.	<500ppm vol.: ± 50 ppm vol. ≥500ppm vol.: ± 10% of ind. vol.
O ₂	0-22% vol.	0.01 vol. %	<2% vol.: ±0.1% vol. ≥2% vol.: ± 5% of ind. vol.

203

204 Important fuel properties of diesel, biodiesel and blends were measured in the
205 laboratory. The instruments used for these measurements and the properties are given
206 in Table 4.

207

Table 4: Important physical properties of test fuels

Properties	Instruments Used	KOME100	KOME50	KOME20	KOME10	Diesel
Viscosity @ 40°C (cSt)	Kinematic Viscometer (Setavis)	4.42	3.51	3.11	3.04	2.78
Density @ 40°C (g/cm ³)	Portable Density Meter (KEM Electronics)	0.881	0.856	0.841	0.836	0.831
Lower Calorific Value (MJ/kg)	Bomb Calorimeter (Parr)	37.98	40.8	42.57	43.18	43.79
Cetane Number	CRF Engine (CI Unit)	50.8	--	--	--	51.2

208

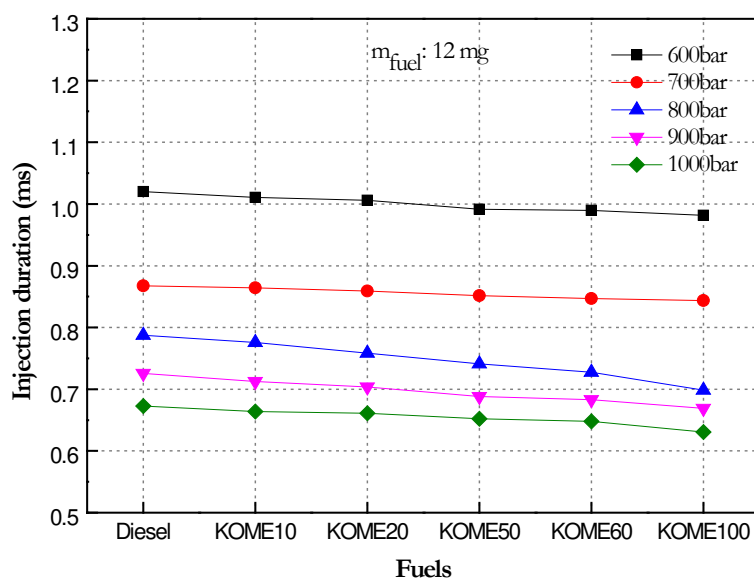
209 **3. Results and Discussion**

210 Effect of fuel injection pressure and SOI timing on engine performance, emissions and
211 combustion characteristics of Karanja biodiesel and blends with mineral diesel
212 (KOME50, KOME20 and KOME10) vis-à-vis baseline mineral diesel were investigated
213 at 1500 rpm speed in a single cylinder research engine. For the sake of clarity, the
214 experiments on Spray are discussed first, followed by the results on engine experiments.

215 **3.1 Injection rate and spray atomization**

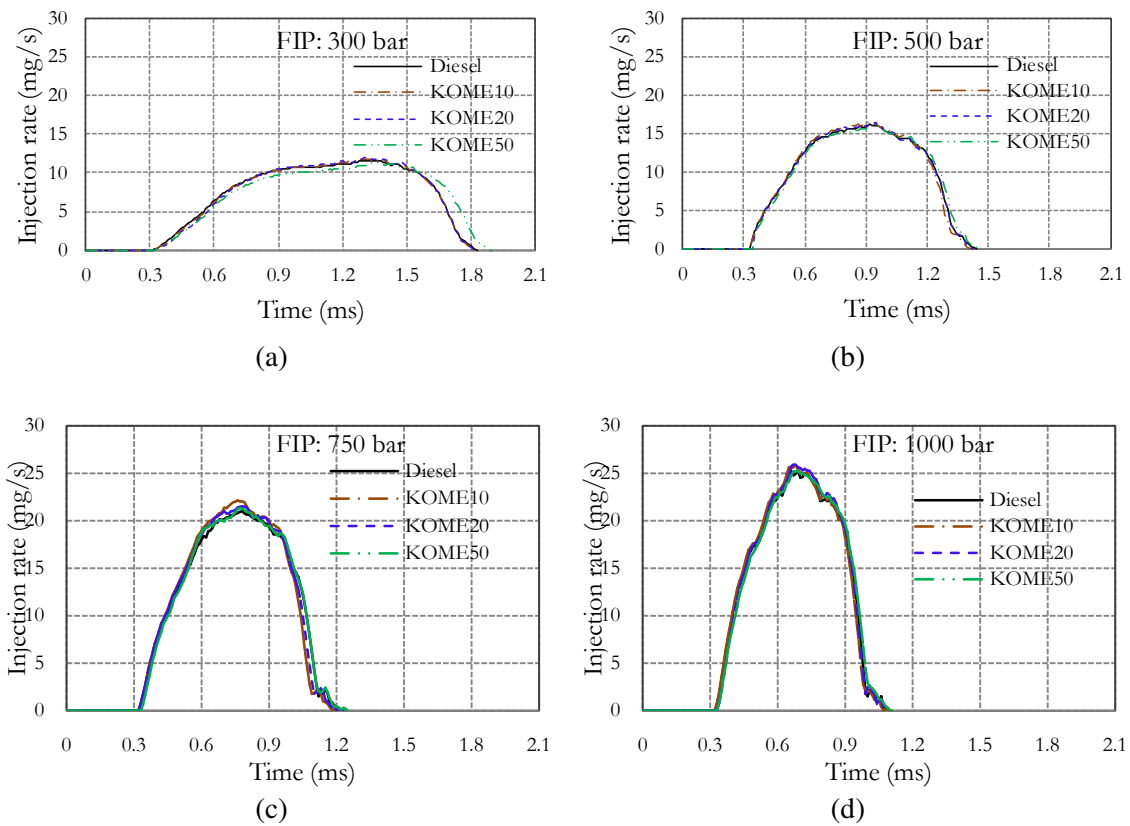
216 Figure 3 shows the effects of fuel injection pressure on the injection duration for
217 different biodiesel blends. As seen from the figure 3, injection duration of KOME blends
218 and mineral diesel decreases with increasing fuel injection pressure. The rate of

219 reduction of injection duration gradually reduced with increasing injection pressure (as
 220 observed for 750 bar and 1000 bar injection pressures). In case of relatively lower
 221 pressures (350 bar and 500 bar), there were large differences between the two injection
 222 pressures compared to that of 750 bar and 1000 bar injection pressures. Therefore for
 223 identical fuel injection quantity, higher injection pressure would require shorter
 224 injection duration because of higher injection velocity from the nozzle exit. This is due to
 225 larger pressure difference between the fuel injection pressure and the ambient pressure
 226 in the engine combustion chamber. On comparing the blending ratio of KOME biodiesel
 227 blends and conventional diesel, the fuel injection duration slightly reduced with
 228 increasing blending ratio of KOME biodiesel blends. Possible reason is that higher
 229 biodiesel blends have higher density due to higher density of biodiesel. Higher density
 230 for higher biodiesel blends results in shorter injection duration however reduction in
 231 rate of injection duration is smaller compared to that of KOME. Boudy *et al.* also
 232 concluded from their modeling results of CRDI system that density of fuel is the main
 233 property, which influences injection parameters greatly such as total injected fuel mass,
 234 pressure wave etc. [1].



235

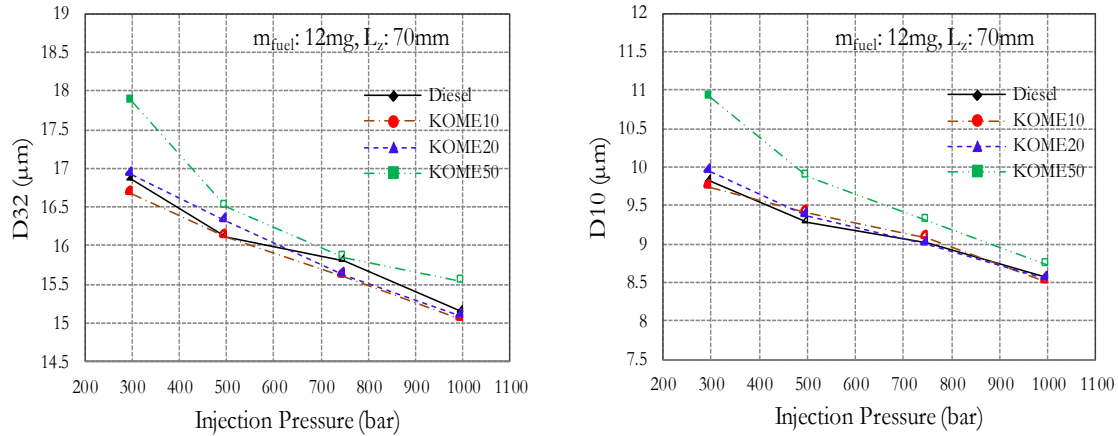
236 Figure 3: Effects of varying fuel injection pressure on the injection duration for different
237 biodiesel blends.



238 Figure 4: Effects of fuel injection pressure on the injection rate for different biodiesel
239 blends at (a) 300, (b) 500, (c) 750 and (d) 1000 bar FIPs.

240 Figure 4 illustrates the effects of fuel injection pressure on the injection rate for
241 different KOME biodiesel blends. As shown in Figure 4, fuel injection duration
242 shortened with increasing injection pressure and the peak injection rate increased with
243 increasing fuel injection pressure.

244 Figure 5 shows the droplet size in the fuel sprays of KOME blends and conventional
245 diesel measured by Phase Doppler Particle Analyzer (PDPA) system. As illustrated in
246 this Figure5, droplet sizes were represented by Sauter mean diameter (SMD or D_{32}) and
247 arithmetic mean diameter (D_{10}) increased with increase in KOME biodiesel
248 concentration in the test blend.



249 (a) Sauter mean diameter

(b) Arithmetic mean diameter

250 Figure 5: Atomization characteristics of KOME blends and diesel fuel

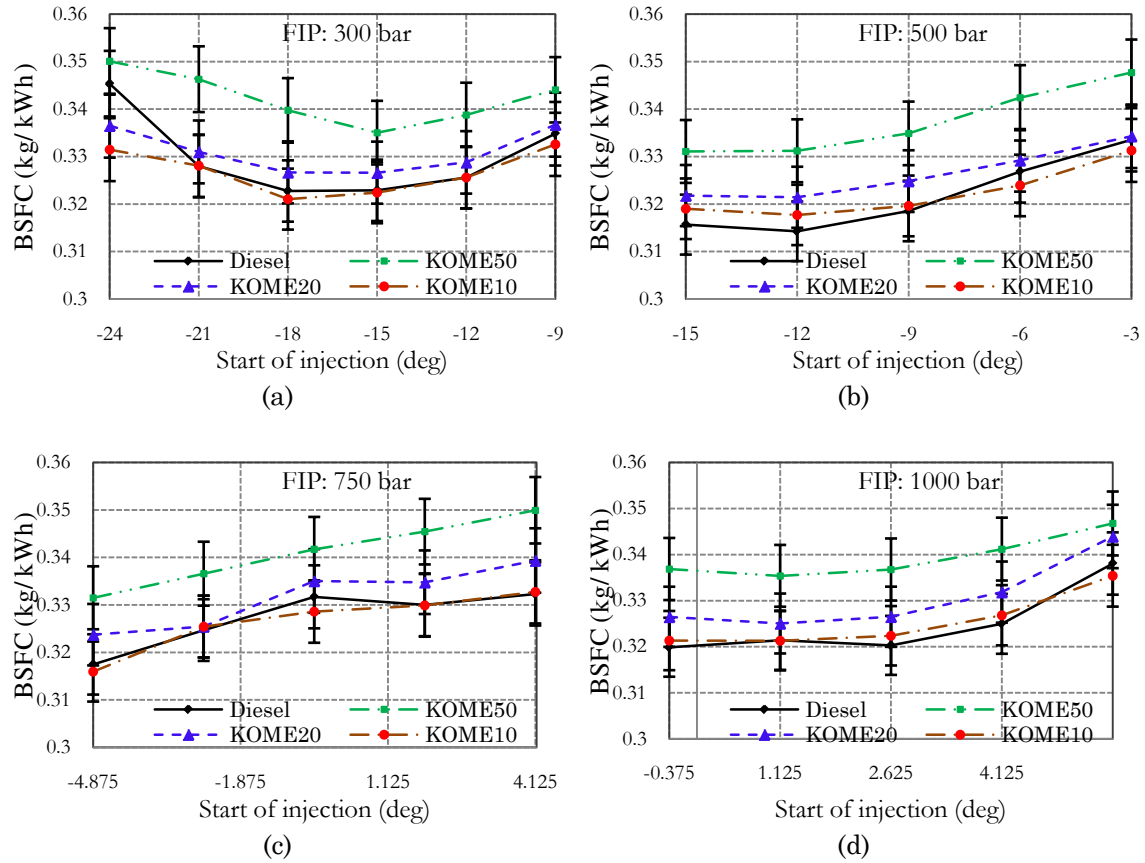
251 Upon comparing the effect of fuel injection pressure on the droplet sizes, one can observe
 252 that the mean diameter of KOME blends and mineral diesel were significantly different
 253 at higher blending ratio due to significantly different fuel density and viscosity. KOME
 254 50 demonstrated significantly larger droplet sizes than mineral diesel as shown in
 255 Figure 5 (a) and (b) [25].

256 3.2 Engine performance characteristics

257 Effects of FIP and SOI timings on engine performance are assessed by comparing the
 258 BSFC and BTE variations vis-a-vis SOI timings for Karanja biodiesel blends and
 259 baseline mineral diesel.

260 *Brake Specific Fuel Consumption*

261 Figure 6 shows the BSFC variation with changing SOI timings in single injection mode
 262 at 300, 500, 750 and 1000 bar FIPs for various blends of Karanja biodiesel vis-à-vis
 263 baseline mineral diesel. Negative values of SOI timings represent start of injection
 264 before top dead center (TDC) (SOI BTDC) and positive values represent start of injection
 265 after the TDC (SOI ATDC).



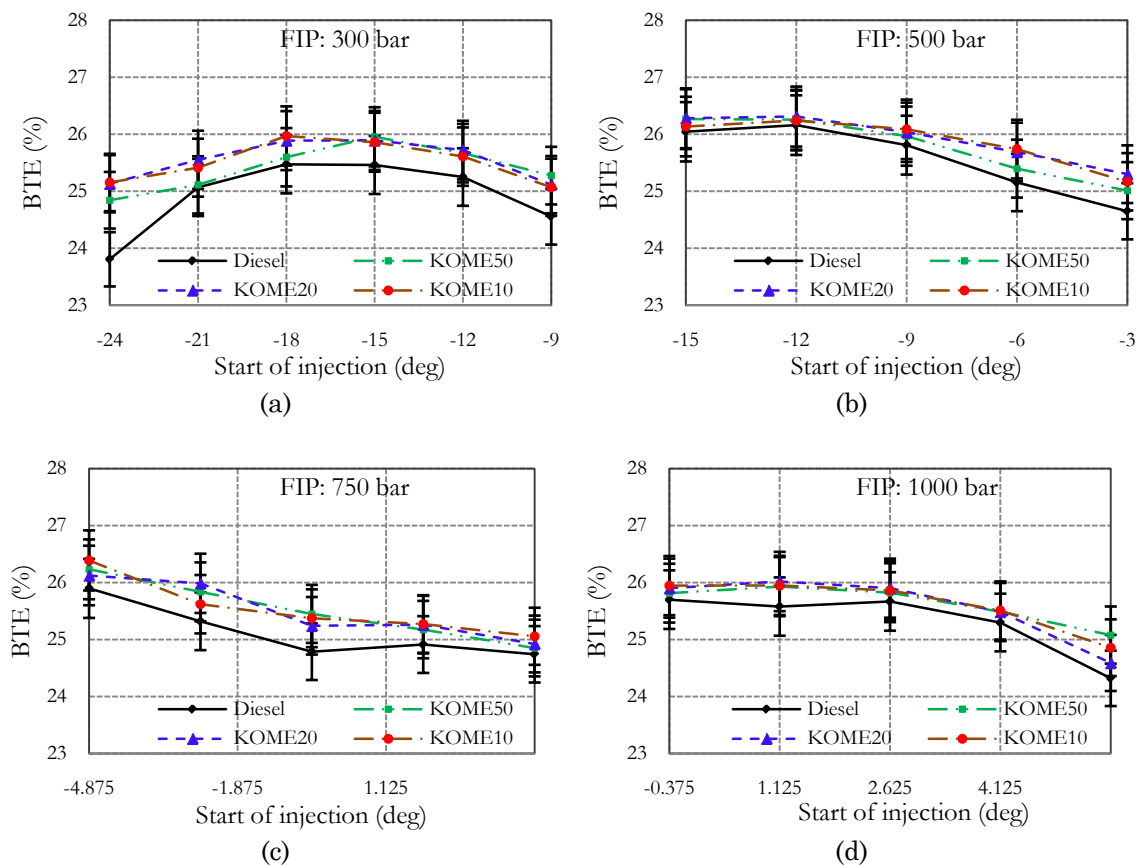
266 Figure 6: Variations in BSFC with varying SOI timings for biodiesel blends vis-à-vis
 267 mineral diesel at (a) 300, (b) 500, (c) 750 and (d) 1000 bar FIPs

268 In single injection mode, BSFC for KOME50 and KOME20 were higher than mineral
 269 diesel (Figure 6). BSFC of KOME10 was almost similar to mineral diesel due to
 270 insignificant difference in physical properties of the test fuels. Reduction of calorific
 271 value of test fuel with increasing concentration of Karanja biodiesel was responsible for
 272 increase in BSFC for KOME50 and KOME20 blends. These results are in conformity
 273 with similar measurement obtained by Yehliu et al. [2], which were primarily due to
 274 approximately 13% lower calorific value of biodiesel compared to mineral diesel. At 300
 275 and 500 bar FIPs, BSFC was lowest at -18°CA and -15°CA SOI timings respectively for
 276 all test fuels. At 750 bar FIP, BSFC was lowest for -4.875°CA SOI timing. At 1000 bar
 277 FIP, BSFC was lowest at 1.125°CA SOI timing for all test fuels. At higher FIPs,
 278 advancement of SOI timings were restricted to -4.875 and -0.375°CA at 750 and 1000
 279 bar FIPs respectively due to very high rate of pressure rise (ROPR). Figure 6 shows that

280 SOI timing corresponding to minimum BSFC retarded with increasing FIP for all test
 281 fuels. Park *et al.* also reported similar findings that at higher FIPs in single injection
 282 mode (600 and 1200 bar); fuel energy was most efficiently converted into useful power,
 283 when SOI timing was closer to TDC [26]. Increasing FIP reduces the injection duration,
 284 leading to finer spray droplets, which improve the air-fuel mixing, thus increasing the
 285 premixed heat release, which results in significant portion of heat being released during
 286 the compression stroke, especially for advanced SOI timings. Higher heat release during
 287 the compression stroke is counter-productive beyond a certain limit because it works
 288 against the piston, which is trying to reach TDC in the compression stroke, hence
 289 minimum BSFC is observed for retarded SOI timings with increasing FIPs.

290 **Brake Thermal Efficiency**

291 Figure 7 shows the variation of BTE of Karanja biodiesel blends with SOI timings at
 292 different FIPs vis-à-vis baseline mineral diesel.



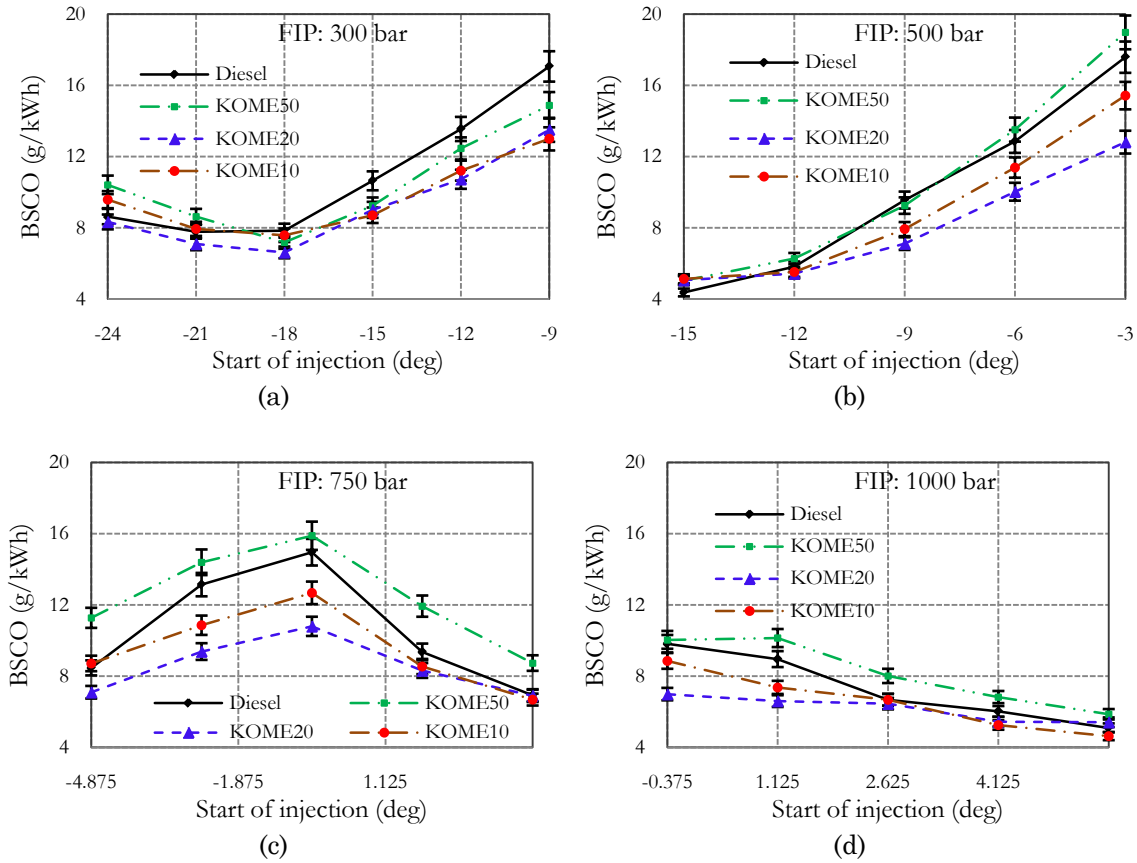
293 Figure 7: Variation in BTE with varying SOI timings for biodiesel blends vis-à-vis
294 mineral diesel at (a) 300, (b) 500, (c) 750 and (d) 1000 bar FIPs

295 Figure 7 shows that the thermal efficiency of Karanja biodiesel blends is higher than
296 mineral diesel at all engine operating conditions. These results are consistent with
297 previous research results [3-6], Suryawanshi et al. also observed increase in BTE for
298 Pongamia biodiesel compared to mineral diesel [3]. Thermal efficiency of lower biodiesel
299 blends (KOME10 and KOME20) was higher than KOME50. BTE was highest at -15°CA
300 SOI timing for all test fuels for 300 and 500 bar FIPs. At a fixed SOI timing, it was
301 observed that increasing FIP generally improves the thermal efficiency of test fuels.
302 Increasing FIP was more effective in increasing BTE of mineral diesel in comparison to
303 Karanja biodiesel blends, which suggests that higher injection pressure is more effective
304 in improving the spray characteristics of fuels with lower viscosity, which is mineral
305 diesel in this case. However, Gumus et al. reported decrease in BTE of mineral diesel
306 with increase in fuel injection pressures from 180 to 240 bar while for biodiesel, found
307 increased with increasing fuel injection pressure at full load [6]. It was also observed
308 that for all test fuels, SOI timing corresponding to maximum BTE shifts towards TDC
309 with increasing FIP. Suryawanshi et al. also reported that retarding injection timing by
310 4° crank angle resulted in minor improvement in thermal efficiency at part loads [3].

311 **3.3 Emissions characteristics**

312 Effect of FIP and SOI timings on carbon monoxide (CO), hydrocarbons (HC) and oxides
313 of nitrogen (NO_x) emissions were investigated by maintaining input fuel energy per
314 cycle constant for all test fuels. Brake specific emissions of regulated gases for Karanja
315 biodiesel blends are compared with mineral diesel for varying fuel injection parameters.

316 ***Carbon Monoxide Emissions***



317 Figure 8: Variations in BSCO emissions with varying SOI timings for biodiesel blends
 318 vis-à-vis mineral diesel at (a) 300, (b) 500, (c) 750 and (d) 1000 bar FIP

319 Figure 8 shows the variations in brake specific carbon monoxide (BSCO) emissions from
 320 Karanja biodiesel blends with varying SOI timings at different FIPs vis-à-vis baseline
 321 mineral diesel. At 300 bar FIP, BSCO emissions were lowest at -18°CA SOI timing for all
 322 test fuels and they increased when injection timing was further retarded (Figure
 323 8(a)). Advanced SOI timings beyond -18°CA resulted in greater formation of fuel rich
 324 zones due to increased ignition delay and relatively inferior atomization of fuel injected
 325 during early phase of fuel injection, when in-cylinder pressure and temperature were
 326 comparatively lower. These fuel rich zones may be the reason for increased CO
 327 emissions. At 500 bar FIP, BSCO emissions were lowest at -15°CA SOI timing which
 328 increased with retarded SOI timings (Figure 8(b)). Retarding the injection resulted in
 329 increase of BSCO as it pushed the majority of combustion into the expansion stroke,
 330 which reduced the temperature and pressure during the later part of the combustion in

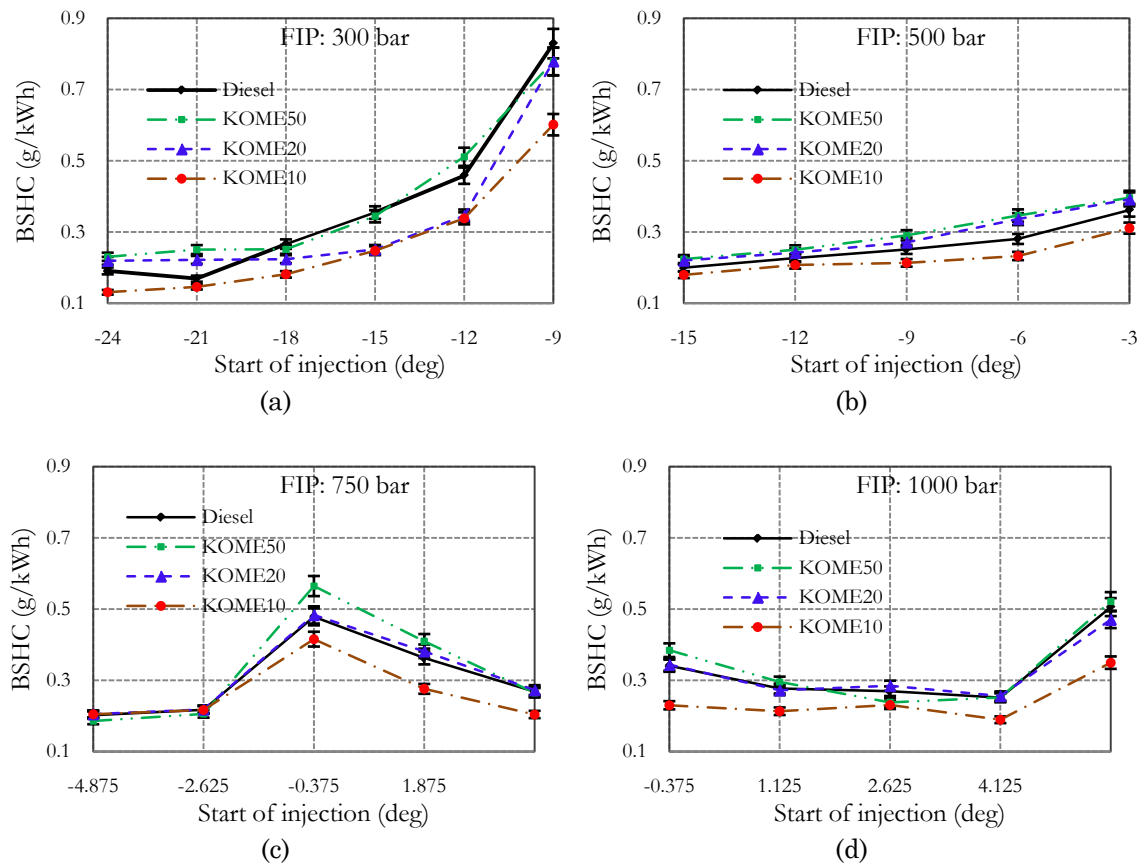
331 the expansion stroke, thus increasing CO formation. Suh *et al.* also observed rapid
332 increase in CO emission for retarded injection timing due to a longer heat release [10].
333 At 750 and 1000 bar FIPs, CO emissions were high when SOI timings were close to TDC
334 and it decreased with retarding SOI timings. This is probably due to wall impingement
335 of high pressure fuel spray droplets. Park *et al.* also reported that injection under high
336 pressure close to TDC results in wall impingement of fuel droplets and/ or accumulation
337 of some fuel in the squish area of the piston [26], which causes relatively inferior mixing
338 of fuel with air, resulting in increased CO and HC emissions. At all FIPs, BSCO
339 emissions of KOME20 and KOME10 were lower than mineral diesel. Similar trends for
340 lower BSCO for biodiesel were also reported by Zhu *et al.* [5]. However, another
341 scientific study by Baldassarri *et al.* reported 10% reduction in CO emissions for B20
342 vis-à-vis mineral diesel [8]. BSCO emissions of KOME50 were higher relative to lower
343 biodiesel blends and at higher injection pressures and they were even higher than
344 mineral diesel. It indicates that higher concentration of Karanja biodiesel in test fuel
345 causes issues related to fuel atomization and mixing, which can possibly offset
346 improvement in the combustion due to oxygenated fuels. At a fixed SOI timing,
347 increasing FIP results in reduction in BSCO emissions due to improvement in fuel-air
348 mixing because of finer fuel spray droplets formation at higher FIP.

349 ***Unburnt Hydrocarbon Emissions***

350 Figure 9 shows the variation in brake specific hydrocarbon (BSHC) emissions of Karanja
351 biodiesel blends vis-à-vis SOI timings at different FIPs in comparison to baseline
352 mineral diesel.

353 BSHC emissions increased with retarded SOI timings for 300 and 500 bar FIPs for all
354 test fuels. Retarding SOI timings lowers the in-cylinder pressure and temperature
355 during combustion, which in-turn increases engine-out HC emissions. At 750 and 1000
356 bar FIPs, BSHC emissions increased sharply, when the SOI timings were close to TDC.

357 This was possibly due to piston wall impingement of the fuel sprays because during the
 358 fuel injection, piston remains very close to the injector tip. Similar increase in HC
 359 emissions levels was also reported by Park *et al.* when SOI timings were close to TDC at
 360 600 and 1200 bar FIPs [26].



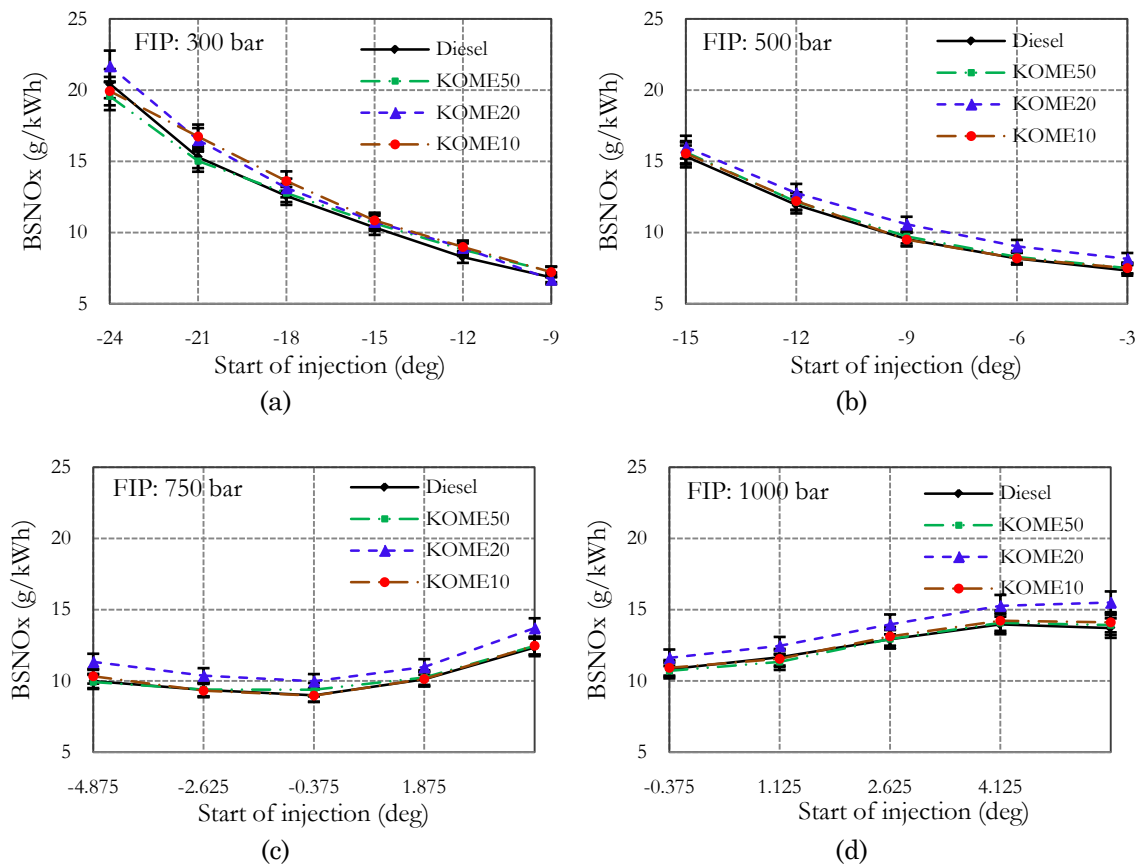
361 Figure 9: Variations in BSHC emissions with varying SOI timings for biodiesel blends
 362 vis-à-vis mineral diesel at (a) 300, (b) 500, (c) 750 and (d) 1000 bar FIPs

363 BSHC emissions start increasing again with further retarded SOI timings at 1000 bar
 364 FIP after 4.125°CA SOI timings (Figure 9(d)) due to lower in-cylinder temperature and
 365 pressure observed during combustion, which increase the formation of unburnt
 366 hydrocarbons. BSHC emissions for KOME10 were lower than mineral diesel but BSHC
 367 emissions of KOME50 and KOME20 were higher than mineral diesel. Ashraful *et al.*
 368 also concluded similar trend of lower HC emission for lower Karanja biodiesel blends in
 369 their review of various experimental studies [20]. It shows that smaller concentrations
 370 of biodiesel improves combustion without adversely affecting the air-fuel mixing

371 significantly however higher concentrations of biodiesel adversely affects the
 372 atomization of the fuel sprays and subsequent air-fuel mixing.

373 *Oxides of Nitrogen Emissions*

374 Figure 10 shows the variations in brake specific NO_x (BSNO_x) emissions vis-à-vis SOI
 375 timings for different FIPs.



376 Figure 10: Variations in BSNO_x emissions with varying SOI timings for biodiesel blends
 377 vis-à-vis mineral diesel at (a) 300, (b) 500, (c) 750 and (d) 1000 bar FIPs

378 At 300 and 500 bar FIPs, BSNO_x emissions decreased with retarded SOI timings for all
 379 test fuels. At 750 and 1000 bar FIPs, BSNO_x emissions were lowest when the SOI
 380 timings were close to TDC but started increasing again when SOI timings were further
 381 retarded after TDC for all test fuels (Figure 10(c)-(d)). It was observed that at these
 382 FIPs, peak of premixed heat release also keeps on increasing, when SOI timings are
 383 retarded upto 4.125 °CA ATDC (Figure 10). Both, peaks of premixed heat release and
 384 BSNO_x concentration reduce when SOI timings were retarded to 5.625 °CA from 4.125

385 °CA. BSNO_x emissions of KOME20 and KOME10 were higher than mineral diesel for
386 all FIPs. NO_x emissions of KOME50 were lower than KOME20 and KOME10 and
387 almost equal to mineral diesel. At BMEP comparable to present study and 450 bar FIP
388 (-3.89 °CA SOI timing), Yehliu *et al.* reported almost comparable BSNO_x emissions [2].
389 These values and trends are consistent with trend of BSNO_x emissions at 500 bar FIP
390 in this study. At the same SOI, increasing fuel injection pressure increases NO_x
391 emissions significantly. Similar trend of NO_x emissions were also reported by Ye et al.
392 [30]. However, Ye et al. also concluded that at the same SOI and fuel injection pressure,
393 biodiesel fueling also increases NO_x emissions significantly. Many studies have reported
394 that effect of biodiesel on NO_x emissions depends on the type of engine used as well as
395 engine operating conditions [2, 27-29]. These trends are observed due to the combined
396 effect of fuel spray characteristics deterioration because of higher fuel viscosity and
397 higher fuel density and differences in the ignition quality due to the differences in the
398 chemical structure of mineral diesel and biodiesel.

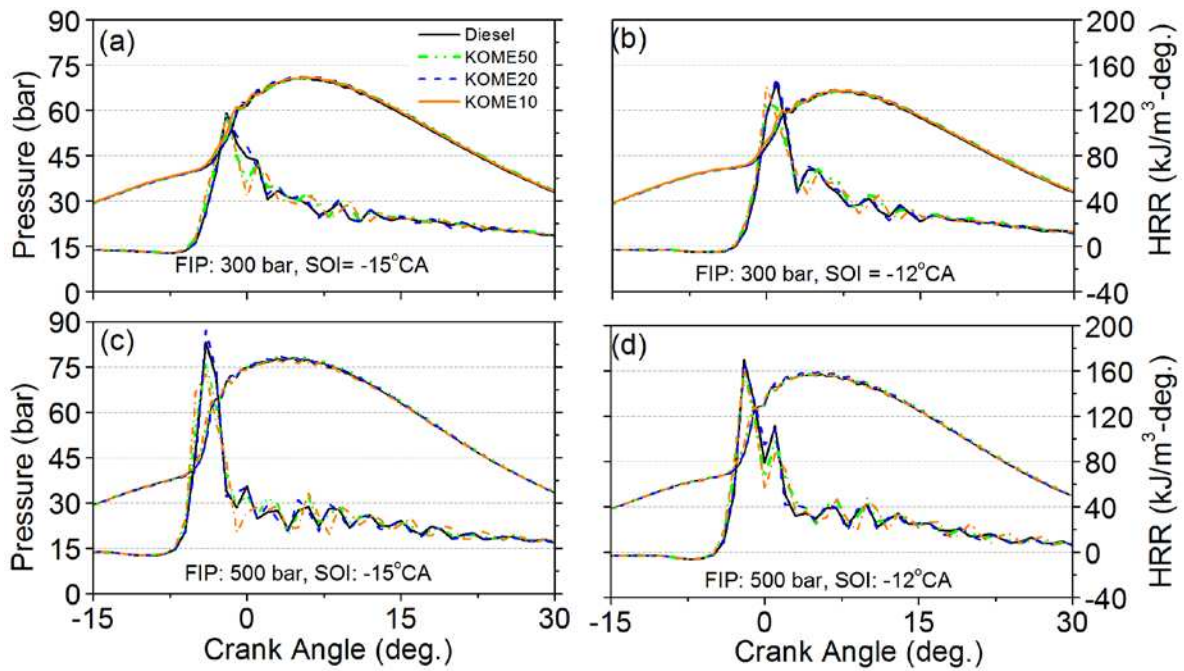
399

400 **3.4 Combustion characteristics**

401 Effects of FIP and SOI timings on the combustion characteristics of KOME50, KOME20
402 and KOME10 vis-à-vis mineral diesel were analyzed by measuring in-cylinder pressure
403 w.r.t. crank angle position in a single cylinder research engine equipped with CRDI fuel
404 injection system. Measured pressure data of 200 consecutive engine cycles were
405 averaged in order to eliminate the effect of cyclic variations of combustion parameters
406 and the experimental data was analyzed to calculate heat release rate (HRR), mass
407 burn fractions (MBF) as well as the combustion duration.

408 ***In-Cylinder Pressure and Heat Release Rate***

409

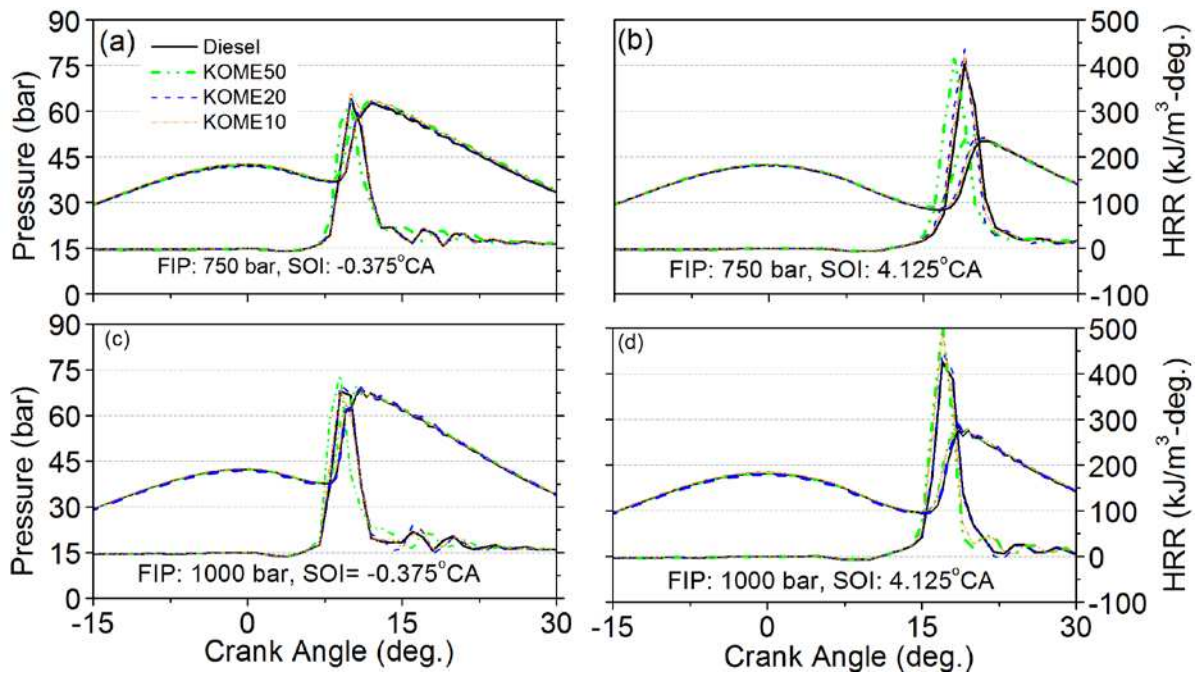


410

411

412 Figure 11: Variation of in-cylinder pressure and HRR with FIP and SOI at 300 and 500
 413 bar FIPs

414 Figure 11 shows the variation of cylinder pressure and HRR at -15 and -12°C SOI
 415 timings at 300 and 500 bar FIPs for Karanja biodiesel blends vis-à-vis mineral diesel.
 416 Negative heat release was observed for all test fuels due to cylinder charge cooling
 417 because of vaporization of the fuel accumulated during the ignition delay period. HRR
 418 becomes positive after the start of combustion (SOC). After the ignition delay, premixed
 419 air-fuel mixture burns rapidly, followed by diffusion combustion, when the HRR is
 420 controlled by rate of air-fuel mixing. Figure 12 shows the variation in in-cylinder
 421 pressure and HRR with SOI timings for higher injection pressures (750 and 1000 bar
 422 FIP) for Karanja biodiesel blends vis-a-vis mineral diesel. For all the test fuels, shift in
 423 in-cylinder pressure and HRR curves is consistent with shift in SOI timings.



424

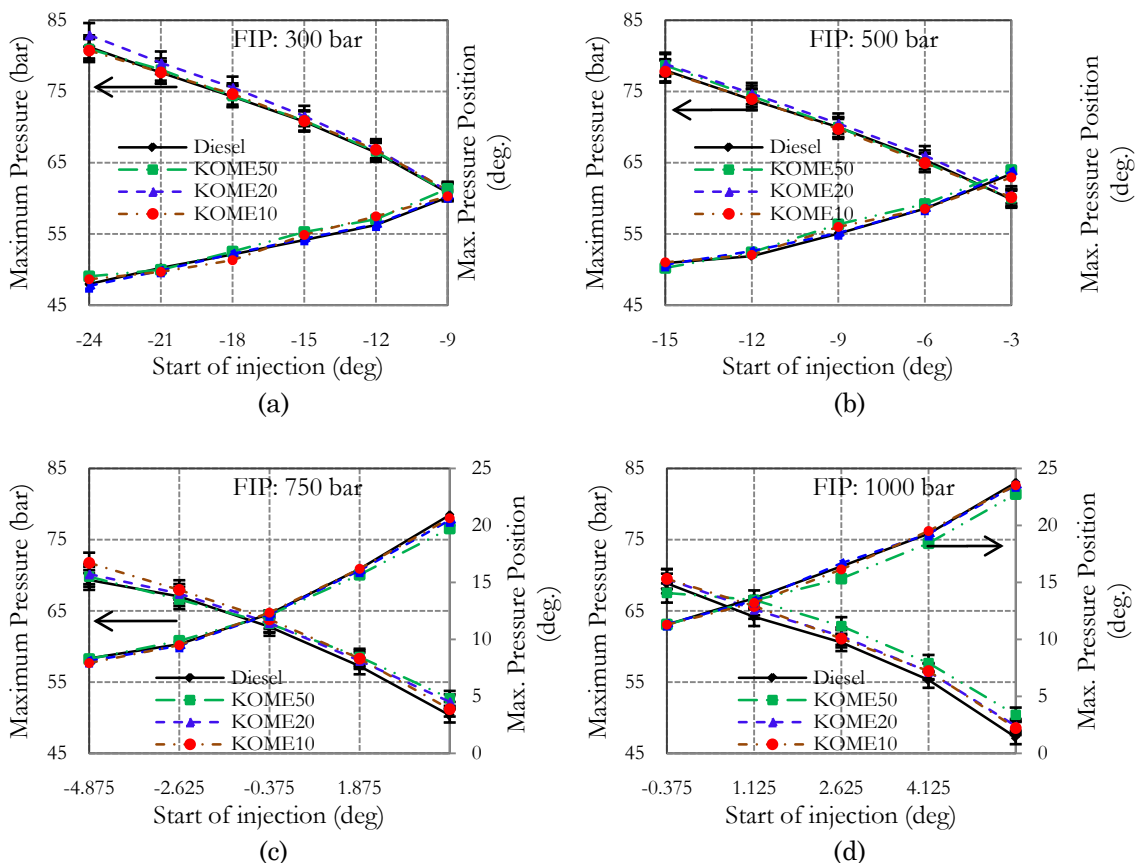
425 Figure 12: Variation of in-cylinder pressure and HRR with FIP and SOI at 750 and 1000
 426 bar FIPs

427 Start of heat release was slightly advanced for KOME10 in comparison to other test
 428 fuels at 300 and 500 bar FIPs and this advancement was higher at advanced SOI
 429 timings (-15° CA SOI timing). Maximum premixed heat release for KOME20 was
 430 comparable to mineral diesel and maximum premixed heat release of KOME50 was
 431 slightly lower than mineral diesel. Reduction in heat release in premixed phase for
 432 biodiesel is also reported by other researchers [30-32]. This is mostly attributed to
 433 biodiesel's lower volatility in addition to the shorter ignition delay [30,32,33]. At higher
 434 FIP and advanced SOI timings (Figure 12), start of combustion advances for KOME50
 435 in comparison to other fuels however at retarded injection timing (figure 12(d)), start of
 436 heat release for KOME50 was comparable to lower Karanja biodiesel blends and
 437 mineral diesel. Ye *et al.* also reported slightly advanced SOC for B40 in comparison to
 438 mineral diesel for SOI timings in the range of -9 to +3° crank angle for varying injection
 439 pressures [30]. Effect of lower volatility of biodiesel and almost comparable cetane

440 number of Karanja biodiesel and mineral diesel may not be significant to alter the HRR
 441 profile of lower biodiesel blends in an engine equipped with CRDI fuel injection system.

442 **Maximum Cylinder Pressure and its Location**

443 Figure 13 shows the variation in maximum cylinder pressure and position of maximum
 444 pressure with SOI timing at 300, 500, 750 and 1000 bar FIPs. For all test fuels,
 445 maximum cylinder pressure decreased and position of maximum pressure retarded with
 446 retarding SOI timings at all FIPs. Retarded position of the peak cylinder pressure with
 447 retarding SOI timings increased the combustion chamber volume at the time of
 448 maximum pressure, which resulted in reduction of peak cylinder pressure for retarded
 449 SOI timings. At 300 bar FIP, maximum cylinder pressure for KOME20 was slightly
 450 higher than other fuels at advanced SOI timings (figure 13(a)).

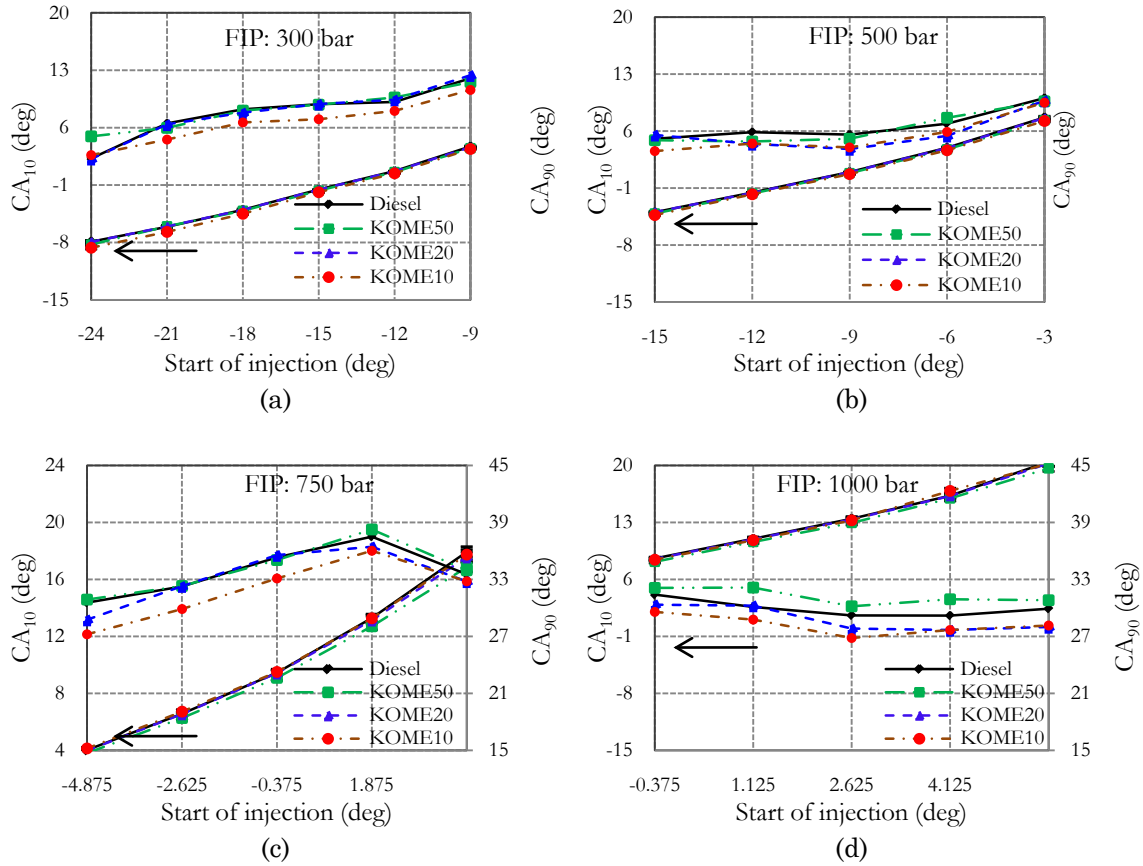


451 Figure 13: Variations in maximum cylinder pressure and its position vis-à-vis SOI
 452 timings for test fuels at (a) 300, (b) 500, (c) 750 and (d) 1000 bar FIPs

453 It can be explained by improvement in combustion due to oxygen content of biodiesel.
454 With higher concentration of biodiesel in the test fuel, this improvement in combustion
455 is offset by inferior spray atomization and poorer mixing characteristics caused by high
456 fuel viscosity and inferior volatility of biodiesel. At retarded SOI timings, maximum in-
457 cylinder pressures of all test fuels were almost same (figures 11). At retarded injection
458 timings, cylinder temperature and pressure were comparatively higher during fuel
459 injection, which improves spray characteristics and reduces the ignition delay for all test
460 fuels, thus reducing the difference in the combustion characteristics of different test
461 fuels. At 750 and 1000 bar FIPs, maximum cylinder pressure of biodiesel increases with
462 increasing biodiesel concentration in the blend at retarded injection timings. At
463 advanced injection timings, maximum cylinder pressure of higher biodiesel blends was
464 comparatively lower (figures 12 (c)-(d)). It shows that higher cylinder pressures and
465 temperatures during the injection improve the spray characteristics of higher viscosity
466 and low volatility fuels. Maximum cylinder pressure increased with increasing FIP at
467 fixed SOI timings for all test fuels due to increased HRR because of improved fuel-air
468 mixing. Suh et al. also observed increased combustion pressure and heat release rate for
469 rapeseed biodiesel blends, when injection pressure were increased to 1000 bar. They
470 concluded that higher fuel injection pressure cause better fuel injection and atomization
471 of higher viscosity biodiesel [10].

472 ***Start and End of Combustion***

473 SOC is characterized by position of 10% MBF in terms of crank angle degree. End of
474 combustion (EOC) is characterized by position of 90% MBF. Figure 14 shows the
475 variations in start and end of combustion with varying SOI timings at 300, 500, 750 and
476 1000 bar FIPs.



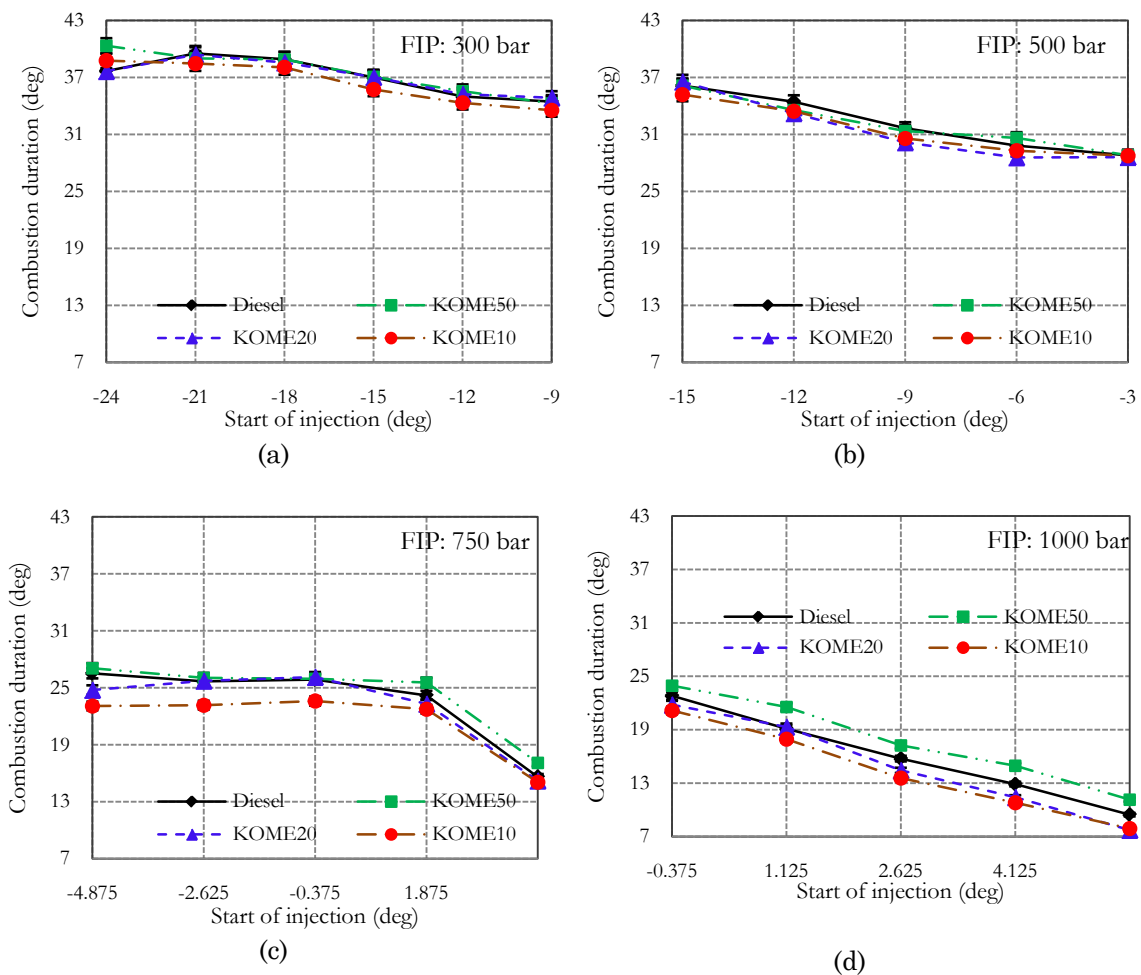
477 Figure 14. Variations in position of 10% and 90% MBF position vis-à-vis SOI timings for
 478 test fuels at (a) 300, (b) 500, (c) 750 and (d) 1000 bar FIP

479 At 300 and 500 bar FIPs, 10% MBF position was almost identical for all test fuels
 480 (Figures 14(a)-(b)). At higher FIPs, SOC was slightly advanced for KOME50 in
 481 comparison to other fuels at all SOI timings (Figures 14(c)-(d)). KOME10 and KOME20
 482 showed earlier EOC in comparison to mineral diesel for all SOI timings. 90% MBF
 483 position of KOME50 was delayed in comparison to mineral diesel and this delay
 484 increased with increasing FIP. It shows that increasing FIP was relatively more
 485 effective in improving the atomization characteristics and mixing of mineral diesel and
 486 lower biodiesel blends. At same SOI timings, SOC advanced with increasing FIP for all
 487 test fuels.

488 **Combustion Duration**

489 Combustion duration is the difference between 90% and 10% MBF positions in terms of
 490 crank angle degrees. Figure 15 shows the variation in combustion duration with SOI

491 timings at 300, 500, 750 and 1000 bar FIPs. It can be observed that combustion duration
 492 decreased with retarding SOI timings for all test fuels at all FIPs. Retarded SOI timings
 493 delayed both start and end of combustion (Figure 14) but delay in SOC timing was
 494 longer in comparison to EOC timing. This longer delay in SOC timing resulted in
 495 shortening of combustion duration with retarded SOI timings. Combustion duration of
 496 KOME10 and KOME20 was shorter than mineral diesel. Combustion duration of
 497 KOME50 was comparable to mineral diesel at 300, 500 and 750 bar FIPs. At 1000 FIP,
 498 combustion duration of KOME50 was higher than mineral diesel.



499 Figure 15. Variations in combustion duration vis-à-vis SOI timings for test fuels at (a)
 500 300, (b) 500, (c) 750 and (d) 1000 bar FIPs

501 Combustion duration decreased with increasing FIP for all test fuels. Lower biodiesel
 502 blends showed faster HRR in comparison to mineral diesel due to fuel oxygen, which

503 also resulted in shorter combustion duration. Higher concentration of biodiesel in test
504 fuels resulted in inferior atomization and fuel-air mixing characteristics due to higher
505 fuel viscosity and inferior volatility characteristics of biodiesel vis-a-vis mineral diesel,
506 which in-turn increased combustion duration of biodiesel blends in the CRDI engine.
507 Similar results of increased combustion duration with increasing biodiesel blend ratio
508 were also observed by CAN. They attributed this behaviour to higher fuel injection
509 duration and slower combustion rate [14].

510 **4. Conclusions**

511 Effects of fuel injection pressure and start of injection timings on CRDI engine
512 performance, emissions and combustion characteristics of Karanja biodiesel (KOME)
513 blends and baseline mineral diesel were investigated at a constant engine speed of 1500
514 rpm, in addition to comprehensive spray investigations were carried out. The fuel
515 injection duration decreased slightly with increasing biodiesel content in the biodiesel
516 blend. Fuel injection duration shortened and peak injection rate increased with
517 increasing fuel injection pressure. Sauter mean diameter and arithmetic mean
518 diameter of fuel spray droplet (D_{32} and D_{10}) decreased with reduction in biodiesel
519 blending ratio due to relatively lower fuel density and viscosity.

520 Brake thermal efficiency of biodiesel blends was slightly higher than mineral diesel.
521 Increasing fuel injection pressures generally improved the thermal efficiency of test
522 fuels. SOI timing corresponding to maximum thermal efficiency was identical for
523 biodiesel blends and mineral diesel. Lower biodiesel blends showed lower BSCO and
524 BSHC emissions in comparison to mineral diesel however BSHC and BSCO emissions
525 were found to be higher for some operating conditions for KOME50. BSNO_x emissions
526 for KOME20 were higher than mineral diesel however they were almost identical to
527 mineral diesel for other blends. Maximum cylinder pressure increased with increasing
528 fuel injection pressure at fixed SOI timing for all test fuels and SOC advanced for lower

529 biodiesel blends in comparison to mineral diesel. For lower biodiesel blends, combustion
530 duration was relatively shorter than mineral diesel but at higher FIPs, combustion
531 duration of KOME50 was found to be relatively longer. These experimental results
532 showed that utilization of upto 10% Karanja biodiesel blends in a CRDI engines can be
533 done for improving engine efficiency and reducing emissions, without any significant
534 hardware changes or ECU recalibration.

535 **Acknowledgements**

536 Research Grant from Department of Science and Technology under Indo-Korea project
537 (No. INT/KOREA/P-04 dated 13-09-2011) is also gratefully acknowledged, which enabled
538 Indian side to undertake this joint research project. Korean side of this research was
539 supported by the National Research Foundation of Korea (NRF) Grant funded by the
540 Korea government (MSIP) (No.20110025295).

541 Support provided by Council of Scientific and Industrial Research (CSIR), Government
542 of India under Senior Research Associate (Pool Scientist) scheme to Mr. Atul Dhar for
543 conducting this research under the supervision of Prof. Avinash Kumar Agarwal at
544 Engine Research Laboratory, IIT Kanpur is gratefully acknowledged.

545 **References**

- 546 1. Boudy F, Seers P, Impact of physical properties of biodiesel on the injection process
547 in a common-rail direct injection system. *Energy Conversion and Management* 2009;
548 50: 2905–2912.
- 549 2. Yehliu K, Boehman AL, Armas O. Emissions from different alternative diesel fuels
550 operating with single and split fuel injection. *Fuel* 2010; 89(2): 423-437.
- 551 3. Suryawanshi JG, Deshpande NV. Effect of injection timing retard on emissions and
552 performance of a pongamia oil methyl ester fuelled ci engine. *SAE Paper* 2005; 2005-
553 01-3677.

- 554 4. Grimaldi CN, Postrioti L, Battistoni M, Millo F. Common rail HSDI diesel engine
555 combustion and emissions with fossil/ bio-derived fuel blends. SAE Paper 2002;
556 2002-01-0865.
- 557 5. Zhu L, Cheung CS, Zhang WG, Huang Z. Emissions characteristics of a diesel engine
558 operating on biodiesel and biodiesel blended with ethanol and methanol. Science of
559 the Total Environment 2010; 408: 914–921.
- 560 6. Gumus M, Sayin C, Canakci M. The impact of fuel injection pressure on the exhaust
561 emissions of a direct injection diesel engine fueled with biodiesel–diesel fuel blends.
562 Fuel 2012; 95: 486-494.
- 563 7. Agarwal AK, Dhar A, Gupta JG, Kim WI, Lee CS, Park SW, Effect of fuel injection
564 pressure and injection timing on spray characteristics and particulate size–number
565 distribution in a biodiesel fuelled common rail direct injection diesel engine, Applied
566 Energy 2014; 130: 212–221.
- 567 8. Baldassarri LT, Battistelli CL, Conti L, Crebelli R, Berardis BD Iamiceli AL,
568 Gambino M, Iannaccone S. Emission comparison of urban bus engine fueled with
569 diesel oil and 'biodiesel' blend. Science of the Total Environment 2004; 327: 147–162.
- 570 9. Kousoulidou M, Fontaras G, Ntziachristos L, Samaras Z . Biodiesel blend effects on
571 common-rail diesel combustion and emissions. Fuel 2010; 89(11): 3442-3449.
- 572 10. Suh HK, Roh HG, Lee CS. Spray and combustion characteristics of biodiesel/diesel
573 blended fuel in a direct injection common-rail diesel engine. Journal of Engineering
574 for Gas Turbines and Power 2008; 130 (3): 1–9.
- 575 11. Wang WG, Lyons DW, Clark NN, Gautam M. Emissions from nine heavy trucks
576 fueled by diesel and biodiesel blend without engine modification. Environmental
577 Science & Technology 2000; 34(6):933 -939.

- 578 12. Kuti OA, Zhu J, Nishida K, Wang X, Huang Z. Characterization of spray and
579 combustion processes of biodiesel fuel injected by diesel engine common rail system.
580 Fuel 2012; <http://dx.doi.org/10.1016/j.fuel.2012.05.014>.
- 581 13. Lee CS, Park SW, Kwon SI, An experimental study on the atomization and
582 combustion characteristics of biodiesel-blended fuels. Energy & Fuels 2005; 19: 2201-
583 2208.
- 584 14. Can Ö, Combustion characteristics, performance and exhaust emissions of a diesel
585 engine fueled with a waste cooking oil biodiesel mixture. Energy Conversion and
586 Management 2014; 87: 676–686.
- 587 15. Ministry of New & Renewable Energy, Government of India; National Policy on
588 Biofuels, http://mnre.gov.in/file-manager/UserFiles/biofuel_policy.pdf accessed on
589 20.05.13.
- 590 16. Sharma YC, Singh B, Upadhyay SN. Advancements in development and
591 characterization of biodiesel: A review. Fuel 2008; 87: 2355–2373.
- 592 17. Agarwal AK, Dhar A. Experimental investigations of performance, emission and
593 combustion characteristics of Karanja oil blends fuelled DIC engine. Renewable
594 Energy 2013; 52: 283-291.
- 595 18. Dhar A, Agarwal AK. Effect of Multiple Injections on Particulate Size-Number
596 Distributions in a Common Rail Direct Injection Engine Fueled with Karanja
597 Biodiesel Blends. SAE Paper 2013-01-1554; 2013.
- 598 19. Kureel RS, Singh CB, Gupta AK, Panday A, Karanja: A potential source of bio-diesel,
599 National Oilseed and Vegetable Oils Development (NOVOD) Board, 2008.
- 600 20. Ashraful AM, Masjuki HH, Kalam MA, Fattah IMR, Imtenan S, Shahir SA,
601 Mobarak HM, Production and comparison of fuel properties, engine performance,
602 and emission characteristics of biodiesel from various non-edible vegetable oils: A
603 review. Energy Conversion and Management 2014; 80: 202–228.

- 604 21. Bosch W. The fuel rate indicator: A new measuring instrument for display of the
605 characteristics of individual injection. SAE Technical Paper 1966; 660749.
- 606 22. Arcoumanis C, Baniasad MS. Analysis of Consecutive Fuel Injection Rate Signals
607 Obtained by the Zeuch and Bosch Methods, SAE Technical Paper 1993; 930921.
- 608 23. Suh HK, Lee CS. Effect of grouped-hole nozzle geometry on the improvement of
609 biodiesel fuel atomization characteristics in a compression ignition engine, Proc.
610 IMechE, Journal of Automobile Engineering 2009; 223: Part D, 1587-1600.
- 611 24. Indian standard IS: 14273, Automotive vehicles – Exhaust emissions – Gaseous
612 pollutants from vehicles fitted with compression ignition engines – method of
613 measurement, 1999, Bureau of Indian Standards, New Delhi, India.
- 614 25. Park SH, Seo HK, Lee CS, Effect of bioethanol-biodiesel blending ratio on fuel spray
615 behavior and atomization characteristics, Energy & Fuel 2009, 23,pp.4092-4098.
- 616 26. Park SH, Yoon SH, Lee CS. Effects of multiple-injection strategies on overall spray
617 behavior, combustion, and emissions reduction characteristics of biodiesel fuel.
618 Applied Energy 2011; 88: 88–98.
- 619 27. Lapuerta M, Armas O, Fernàndez JR. Effect of biodiesel fuels on diesel engine
620 emissions. Progress in Energy and Combustion Science 2008; 34:198–223.
- 621 28. Miyamoto, N, Ogawa, H, Nurun, NM, Obata, K, Arima, T. Smokeless, low NO_x, high
622 thermal efficiency, and low noise diesel combustion with oxygenated agents as main
623 fuel. SAE paper 1998; 980506.
- 624 29. Lešnik L, Iljaz J, Hribernik A, Kegl B, Numerical and experimental study of
625 combustion, performance and emission characteristics of a heavy-duty DI diesel
626 engine running on diesel, biodiesel and their blends. Energy Conversion and
627 Management 2014; 81: 534–546.

- 628 30. Ye P, Boehman AL. An investigation of the impact of injection strategy and biodiesel
629 on engine NO_x and particulate matter emissions with a common-rail turbocharged
630 DI diesel engine. *Fuel* 2012; 97: 476-488.
- 631 31. Szybist JP, Kirby SR, Boehman AL. NO_x emissions of alternative diesel fuels: a
632 comparative analysis of biodiesel and FT diesel. *Energy & Fuels* 2005; 19: 1484–
633 1492.
- 634 32. Yu CW, Bari S, Ameen A. A comparison of combustion characteristics of waste
635 cooking oil with diesel as fuel in a direct injection diesel engine. *Proceedings of the*
636 *Institution of Mechanical Engineers, Part D: Journal of Automobile Engineering*
637 2002; 216: 237–243.
- 638 33. Sun J, Caton JA, Jacobs TJ. Oxides of nitrogen emissions from biodiesel-fuelled
639 diesel engines. *Progress in Energy and Combustion Science* 2010; 36: 677-695.